Geomorphic Controls on Cascading Flood–Landslide Multi-Hazard Susceptibility Revealed by Machine Learning and Explainable AI in a Fragile Biodiversity Hotspot of India

Sabirul Sk[1], Nirul Ranjan Patra[2], Subimal Ghosh[3], Subhankar Karmakar[1, 2]
[1]Centre for Climate Studies, Indian Institute of Technology Bombay, Mumbai 400076, India
[2]Environmental Science and Engineering Department, Indian Institute of Technology Bombay, Mumbai 400076, India
[3]Department of Civil Engineering, Indian Institute of Technology Bombay, Mumbai 400076, India
Email of first and corresponding author: sabirul@iitb.ac.in/ sabirulgis@gmail.com
Email of co-authors: nirul.iiserb@gmail.com; subimalghosh@gmail.com; subhankar.karmakar@gmail.com

Abstract

Floods and landslides frequently co-occur in steep tropical mountain belts, generating cascading hazards that threaten human societies and fragile ecosystems. The Western Ghats (WG) of India, a globally recognised biodiversity hotspot and one of the most monsoon-affected regions in the tropics, are highly susceptible to such compound events. However, the geomorphic controls linking floods and landslides remain poorly quantified at regional scales. Here, we develop the first integrated flood–landslide multi-hazard susceptibility framework for the WG by utilising high-resolution digital elevation model-derived geomorphic descriptors with multi-decadal hazard inventories. Six machine-learning models are evaluated, and an ensemble of XGBoost, LightGBM, and CatBoost yields the highest predictive performance for both hazards. Explainable AI highlighting flood susceptibility (FS) is primarily associated with downslope index, convexity, geomorphic flood index, and overland-flow distance, whereas landslide susceptibility (LS) is strongly influenced by structural lineaments, flow accumulation, stream power, and plan curvature. Spatial analysis reveals distinct regional hotspots where geomorphic conditions promote the co-occurrence of floods and landslides across parts of Maharashtra, Kerala, and Karnataka states. Extreme rainfall analysis further identifies the IMD-defined very heavy rainfall threshold (115.6 mm day^{-1}) as a critical trigger beyond which cascading hazard intensity increases sharply. Overall, the results demonstrate that geomorphology provides a robust predictive template for cascading flood–landslide hazards and underscore the importance of terrain-informed early-warning systems and sustainable land-use planning in fragile mountain regions.

Keywords: Digital elevation model, flood susceptibility, geomorphic descriptors, landslide susceptibility, machine learning, multi-hazard, Western Ghats

1 INTRODUCTION

Extreme precipitation in mountainous regions frequently triggers cascading hydrogeomorphic hazards, including landslides and flooding (Acosta-Quesada and Quesada-Román, 2024; Deijns et al., 2024; Mani et al., 2023). These processes are tightly coupled: intense rainfall, steep slopes, saturated soils, and confined channels interact to amplify impacts beyond those of individual hazards (Kappes et al., 2012; Kharismalatri et al., 2025; Leonard et al., 2014). Under climate change, increasing rainfall intensity in tropical mountain belts is expected to intensify such compound events (Encalada et al., 2019).

The geomorphic response of mountain catchments is governed by terrain configuration, lithology, structural discontinuities, and sediment connectivity (Mani et al., 2023). These controls regulate whether rainfall generates slope failure, rapid runoff and flooding, or coupled flood–landslide cascades (Arango-Carmona et al., 2025; Croissant et al., 2017; Fan et al., 2025; Zhang et al., 2024). In humid tropical mountains, strong hillslope–channel connectivity promotes sediment delivery that alters channel morphology, while flood undercutting destabilises saturated slopes (Rusk et al., 2022). Despite their significance, regional-scale quantification of these geomorphic–hydrological linkages remains limited.

The Western Ghats (WG) of India represent a highly susceptible monsoon-dominated escarpment (Encalada et al., 2019). The 2018 Kerala disaster illustrated the coupled nature of flood–landslide processes under prolonged extreme rainfall (Hao et al., 2020; Tripathy et al., 2020). However, most regional assessments treat floods and landslides independently, overlooking shared terrain controls.

Recent advances in machine learning (ML) and deep learning (DL) offer new opportunities to characterise such complex, nonlinear hazard systems (Liu et al., 2025; Luo et al., 2025; Rusk et al., 2022). ML models have shown strong predictive skill for individual hazards, including floods and landslides (Deijns et al., 2024; Deroliya et al., 2022; Ibebuchi and Abu, 2025), while DL approaches can capture latent spatial patterns and interactions among geomorphic and hydrological variables (Pourghasemi et al., 2020; Tiggeloven et al., 2025; Ullah et al., 2022; Wang et al., 2020; Youssef et al., 2023). However, ML- and DL-based multi-hazard susceptibility assessments remain limited, particularly in monsoon-dominated mountain belts where compound flood–landslide processes are frequent and highly damaging.

Here, we develop a geomorphologically informed multi-hazard susceptibility framework for the WG. Specifically, we: (i) derive DEM-based geomorphic drivers conditioning both hazards; (ii) model flood and landslide susceptibility using ML; (iii) integrate outputs to map compound hotspots; and (iv) evaluate rainfall exceedance thresholds activating cascading hazard zones. This study links terrain configuration with rainfall forcing to improve terrain-informed risk assessment in humid tropical mountains.

2 STUDY AREA AND DATA

2.1 Study Area

The Western Ghats (WG), also known as the Sahyadri Mountains, form a 1,600 km orographic escarpment along India's southwest coast (8°–21°N) (Encalada et al., 2019). Elevations exceed 2,500 m, generating strong monsoon–orographic interactions (Fig.1). Steep slopes, deep valley incision, and structurally weakened bedrock contribute to recurrent floods, landslides, and cascading hazard interactions (Das, 2020).

.

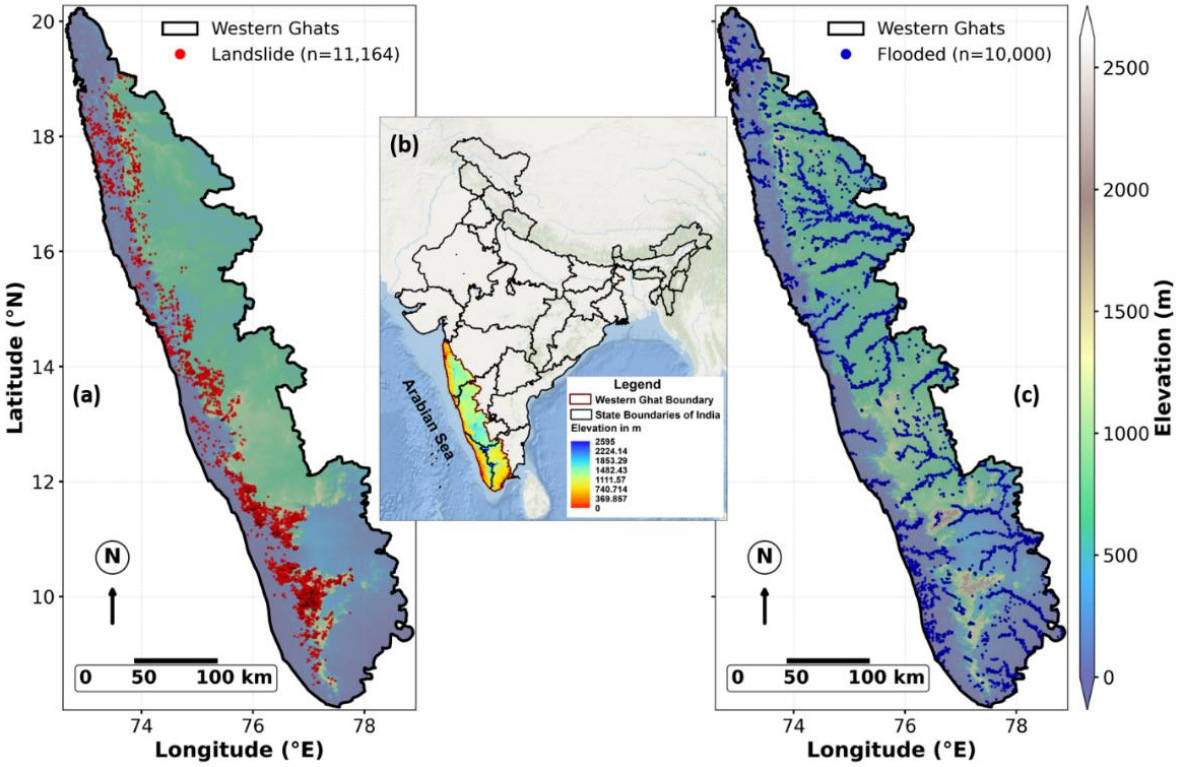

Figure 1. Location map of the Western Ghats (WG) mountain range and the spatial distribution of observed hazards. (a) Elevation map of the WG overlaid with documented landslide occurrences (n = 11,164) obtained from the Geological Survey of India. (b) Regional context map showing the position of the Western Ghats along the western margin of India, spanning the states of Maharashtra, Goa, Karnataka, Kerala, and Tamil Nadu. (c) Elevation map overlaid with observed flood-affected locations (n = 10,000), illustrating the distribution of recent flood impacts across the WG.

2.2 Data

2.2.1 Geomorphic and Geological Data

We derived a suite of geomorphic descriptors from the 90-m hydrologically corrected Shuttle Radar Topography Mission (SRTM) DEM, including slope, relief, curvature, LS factor, topographic wetness index, flow accumulation, multi-resolution valley bottom flatness, valley depth, ridge–valley distance, and terrain ruggedness. These metrics capture hydrologic convergence, slope stability, and geomorphic confinement, which are relevant to both flood and landslide processes (Bernard et al., 2022; Deroliya et al., 2022; Luo et al., 2025; Pourghasemi et al., 2020; Rusk et al., 2022; Ullah et al., 2022; Youssef et al., 2023). Geological and structural datasets from the Geological Survey of India (GSI; https://bhukosh.gsi.gov.in/Bhukosh) were integrated, including lithology, faults, thrusts, lineaments, and regolith units. All vector layers were rasterised to 90-m resolution. Distance-to-fault and lineament-density surfaces were computed to represent structural weakening.

2.2.2 Hazard Inventories

Flood occurrence was derived from the Global Flood Database (2000–2018) (https://global-flood-database.cloudtostreet.ai/), generating a binary presence–absence layer. Landslide inventories (2010–2021) were compiled from NRSC and GSI datasets and rasterised to 90 m resolution.

3 METHODS

Figure 2 shows the overall methodological workflow adopted in this study, outlining the complete sequence from data acquisition and pre-processing to predictor selection, ML model development, and susceptibility map generation. The framework integrates multi-source geospatial datasets, DEM-derived geomorphic descriptors, geological and structural information, and long-term hazard inventories to produce high-resolution flood and landslide susceptibility models for the WG. The major components of the methodology are described below.

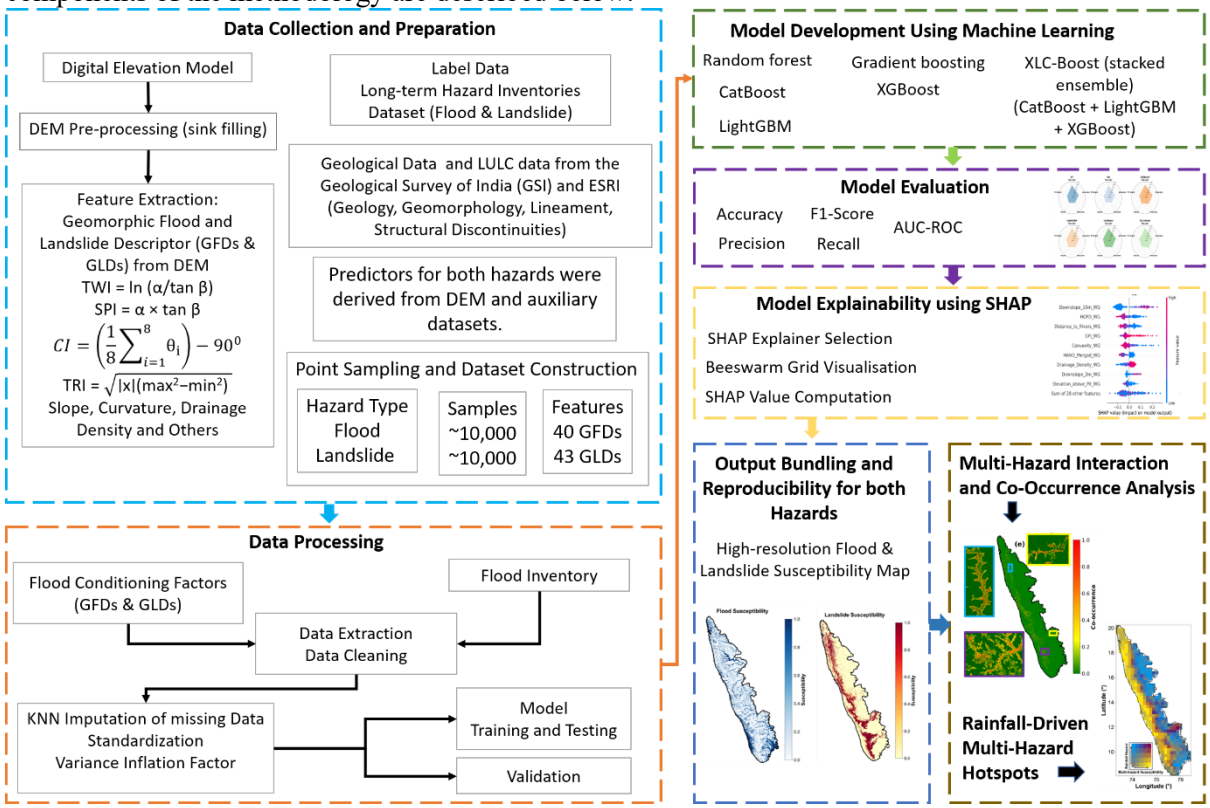

Figure 2. Overall methodological workflow for developing flood and landslide susceptibility models in the WG. The framework integrates multi-source geospatial datasets, geomorphic conditioning factors, long-term hazard inventories, and ML modelling to derive high-resolution susceptibility maps.

Predictor Selection and Multicollinearity Assessment

To reduce redundancy and avoid unstable model behaviour, we quantified multicollinearity among predictors using the Variance Inflation Factor (VIF) (Deroliya et al., 2022; Mansfield and Helms, 1982):

$$VIF = \frac{1}{1-R_i^2} \quad (1)$$

where R_i^2 is the coefficient of determination when predictor i is regressed against all other predictors. Higher VIF values indicate stronger collinearity, which can inflate model variance and distort the relative influence of predictors. A threshold of VIF < 2 was applied for landslides and VIF < 5 for floods. After iterative filtering, 33 flood predictors and 29 landslide predictors were retained (Fg.3).

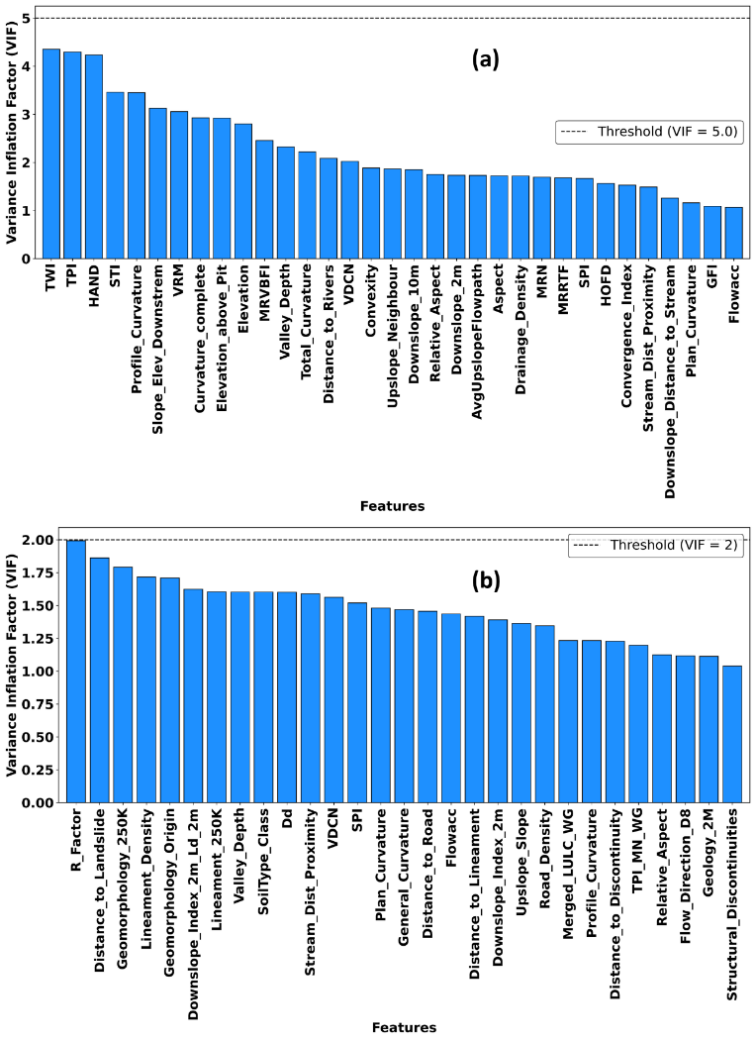

Figure 3. Variance Inflation Factor (VIF) analysis for flood (a) and landslide (b) geomorphic drivers. For the flood dataset, 40 initial predictors were screened using a VIF threshold of 5, resulting in a reduced set of 33 non-collinear variables. For the landslide dataset, 43 geomorphic and geological drivers were evaluated using a stricter VIF threshold of 2, yielding 29 retained indicators. Dashed horizontal lines denote the respective VIF thresholds.

Machine-Learning-Based Susceptibility Modelling

Flood and landslide susceptibility were modelled independently using Random Forest, Gradient Boosting, XGBoost, LightGBM, CatBoost, and a soft-voting ensemble (XLC-Boost) (Murphy, 2013; Waleed and Sajjad, 2025). Spatially balanced sampling and a 70/30 spatially stratified train–test split were applied (Rusk et al., 2022). The ensemble susceptibility was computed as:

$$S_{ensemble} = \frac{S_{Cat} + S_{XGB} + S_{LGBM}}{3} \quad (2)$$

where S_{Cat}, S_{XGB}, and S_{LGBM} denote the susceptibility scores estimated by the CatBoost, XGBoost, and LightGBM models, respectively, each representing the model-estimated probability of a location being susceptible to the corresponding hazard. Model performance was evaluated using the area under the receiver operating characteristic curve (ROC–AUC) and confusion-matrix-based metrics.

Multi-Hazard Susceptibility

To characterise cascading or concurrent hazard potential, we combined flood susceptibility (FS) and landslide susceptibility (LS) using three formulations:

$$MH_{mean} = (LS + FS)/2 \quad (3)$$

$$MH_{max} = \max(LS, FS) \quad (4)$$

$$MH_{prod} = LS \times FS \quad (5)$$

The product index (MH_{prod}) highlights areas where both hazards co-occur with high intensity, a diagnostic for cascading hazard pathways.

Rainfall Data and Exceedance Analysis

Daily India Meteorological Department (IMD) rainfall (1982–2021) was used to compute the exceedance probability of Very Heavy Rainfall (≥115.6 mm/day) (IMD, 2021; Pai et al., 2014). Exceedance probability was calculated as the proportion of days exceeding this threshold. A bivariate choropleth was constructed by jointly mapping rainfall exceedance probability and multi-hazard susceptibility to identify rainfall–terrain activation zones.

4 RESULTS

Model Performance

All machine learning algorithms demonstrated strong predictive performance for both flood and landslide susceptibility (Fig. 4). For floods, XLC-Boost achieved the highest discrimination (AUC = 0.945), followed closely by XGBoost (0.943), CatBoost (0.943), and LightGBM (0.941). Random Forest (0.929) and Gradient Boosting (0.924) showed slightly lower but robust performance. For landslides, performance was higher overall, with XLC-Boost achieving an AUC of 0.988 and all boosting-based models exceeding 0.98. Random Forest and Gradient Boosting achieved AUC values of 0.984 and 0.981. These results indicate strong and stable classification across hazards under spatial validation.

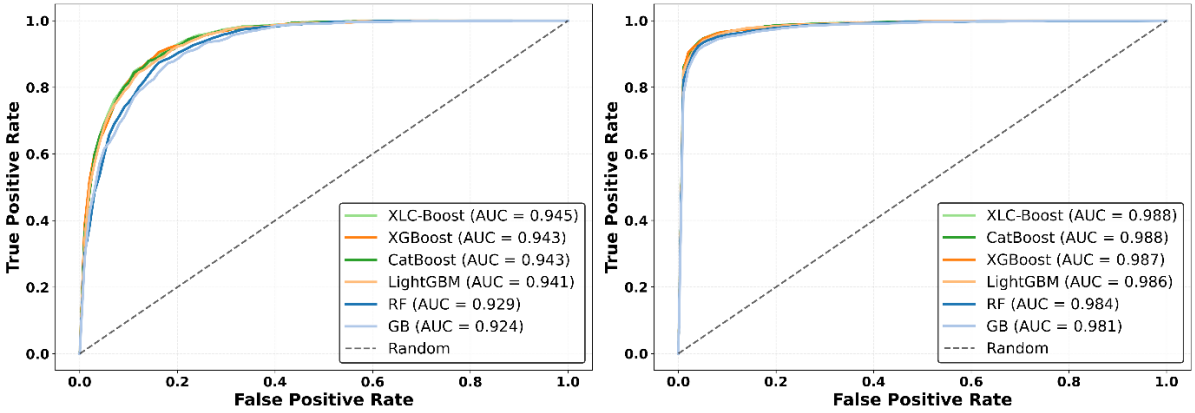

Figure 4. Receiver Operating Characteristic (ROC) curves showing the predictive performance of six machine learning algorithms for flood susceptibility (left) and landslide susceptibility (right) in the Western Ghats. Boosting-based models demonstrate the highest discrimination ability, with XLC-Boost achieving the best performance for floods (AUC = 0.945) and landslides (AUC ≈ 0.988). Random Forest and Gradient Boosting show slightly lower but still strong predictive skill. The dashed line represents random classification.

Flood and Landslide Susceptibility Patterns

The flood and landslide models reveal distinct yet complementary spatial patterns (Fig. 5). Landslide susceptibility concentrates along steep escarpments, deeply incised valleys, and structurally weakened

bedrock, particularly in Idukki, Wayanad, central Kerala, and interior Karnataka (Fig. 5a). In contrast, flood susceptibility highlights hydrologically convergent valleys and low-relief basin floors, with pronounced hotspots in Alappuzha, Thrissur, Ernakulam, and river floodplains of Maharashtra (Fig. 5b). These contrasting patterns reflect the different geomorphic settings predisposing the landscape to each hazard.

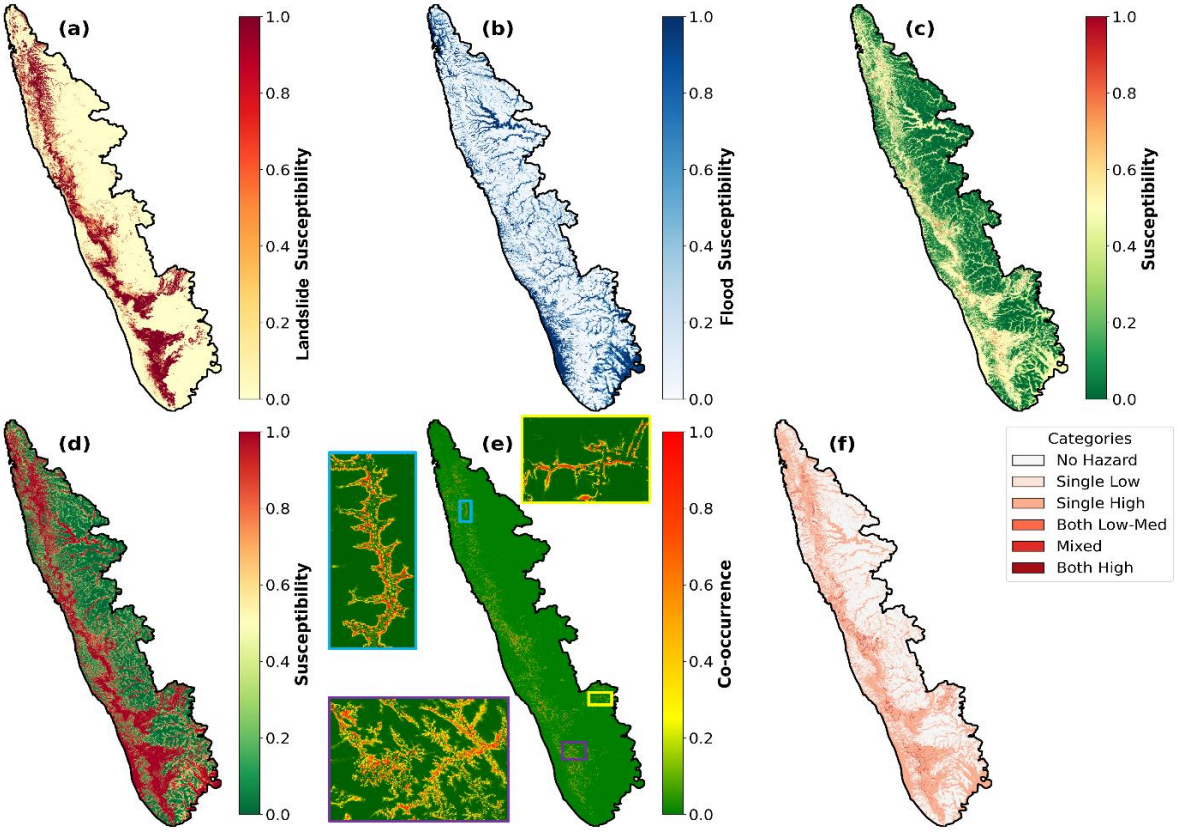

Figure 5. Flood, landslide, and multi-hazard susceptibility across the Western Ghats. (a) & (b) Landslide and flood susceptibility map derived from high-resolution geomorphic and geological descriptors. (c) Mean multi-hazard surface showing areas where both hazards maintain moderate–high susceptibility. (d) Maximum hazard envelope representing the dominant hazard at each pixel. (e) Multiplicative co-occurrence index highlighting zones where flood and landslide susceptibility simultaneously intensify; insets show fine-scale channel–hillslope coupling. (f) Categorical multi-hazard classification delineating six compound hazard states ranging from no hazard to "both high." Together, these panels identify spatial hotspots where steep slopes, structural discontinuities, and concentrated monsoon runoff interact to produce cascading multi-hazard risk.

Multi-Hazard Co-occurrence and Cascading Hotspots

Multi-hazard metrics reveal clear spatial interaction between floods and landslides. The mean surface (Fig. 5c) identifies regions where moderate-to-high susceptibility overlaps, particularly along hillslope–channel interfaces. The multiplicative co-occurrence index (Fig. 5e) isolates cascading hotspots in Idukki, parts of Wayanad, northern Kerala, and the high-relief belts of Karnataka. These zones align with areas where steep slopes intersect confined drainage networks, indicating strong terrain-driven coupling. The categorical classification (Fig. 5f) shows that "Both High" zones are spatially restricted to regions combining extreme relief, structural discontinuities, and concentrated runoff, confirming that geomorphology governs cascading hazard amplification.

Geomorphic Controls and Rainfall Triggering of Cascading Hazards

SHapley Additive exPlanations (SHAP) demonstrates contrasting controls for each hazard (Fig. 6). Flood susceptibility is dominated by hydrologic convergence metrics (downslope index, drainage density, geomorphic flood index), whereas landslides are strongly influenced by slope steepness, rainfall erosivity, curvature, and structural indicators. The consistency of dominant predictors across algorithms confirms robust geomorphic control.

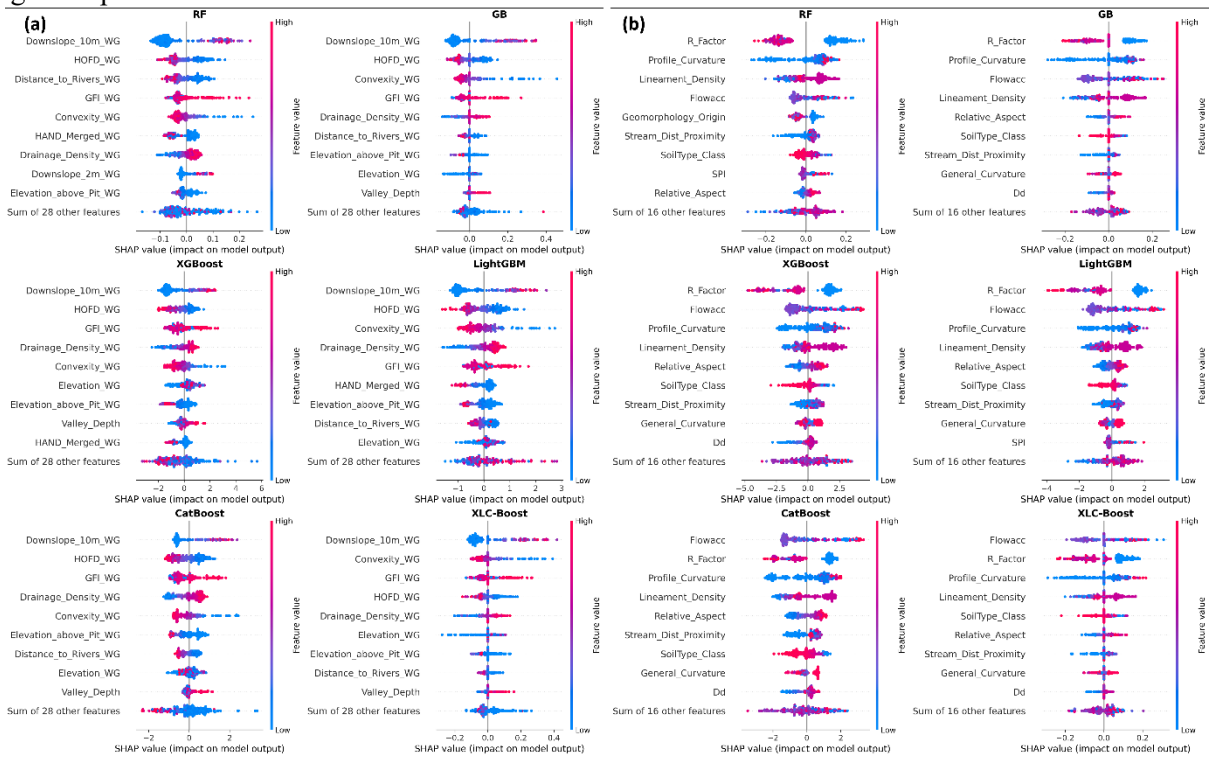

Figure 6. SHAP-based feature importance for flood (a) and landslide (b) susceptibility models across six machine-learning algorithms.

Extreme rainfall analysis identifies 115.6 mm/day (IMD “very heavy rainfall”) as a critical activation threshold. The bivariate rainfall–multi-hazard map (Fig. 7) shows strong spatial coupling between high rainfall exceedance and elevated multi-hazard susceptibility, particularly in the southern and central Western Ghats. Areas with low rainfall exceedance correspond to predominantly low multi-hazard intensity, indicating that extreme rainfall acts as a climatic trigger superimposed on terrain predisposition.

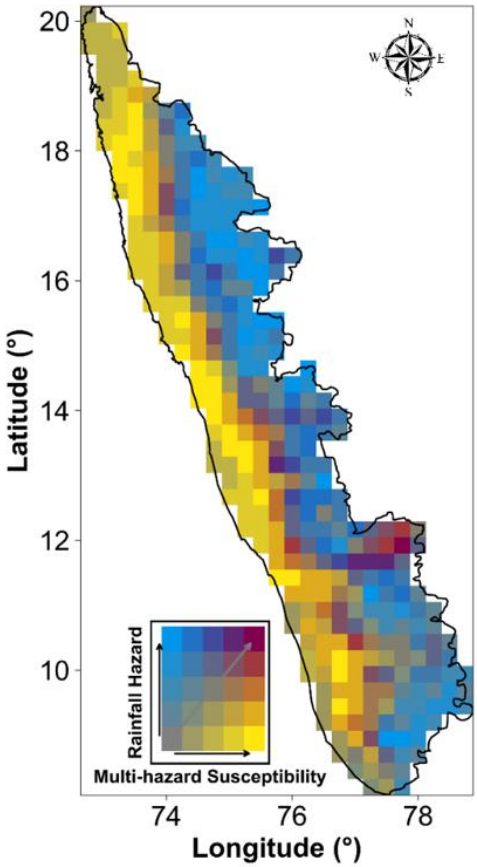

Figure 7. Bivariate rainfall–multi-hazard map for the Western Ghats. The 2D colour space shows how multi-hazard susceptibility varies with increasing rainfall hazard. Warmer colours indicate areas where very heavy rainfall coincides with high flood–landslide susceptibility, highlighting climatically triggered multi-hazard hotspots across southern and central Western Ghats.

5 DISCUSSION

This study shows that cascading flood–landslide hazards in the Western Ghats arise from the spatial alignment of geomorphic predisposition and extreme monsoon rainfall. Steep slopes, valley incision, and litho-structural discontinuities promote landsliding (Youssef et al., 2023; Zhang et al., 2024), while hydrologic convergence and drainage confinement enhance flood susceptibility (Das, 2020; Deroliya et al., 2022). Where these controls overlap, particularly along hillslope–channel interfaces, distinct multi-hazard hotspots emerge across Idukki, Wayanad, and the central escarpment.

SHAP-based analysis reveals contrasting yet complementary controls: floods are primarily governed by flow routing and accumulation (Ibebuchi and Abu, 2025; Li et al., 2025; Waleed and Sajjad, 2025), whereas landslides respond strongly to slope steepness and structural weakening (Liu et al., 2025; Pradhan et al., 2023; Youssef et al., 2023). Their interaction is intensified where steep terrain directly connects to hydrologically active channels, facilitating cascading processes.

Extreme rainfall acts as a nonlinear trigger superimposed on terrain susceptibility. Exceedance of the IMD very heavy rainfall threshold (115.6 mm/day) corresponds to a sharp increase in multi-hazard intensity, consistent with observations from the 2018 Kerala event (Hao et al., 2020; Tripathy et al., 2020). . These findings indicate that extreme rainfall preferentially activates hazards in geomorphically predisposed terrain rather than uniformly across the landscape.

Despite the strong predictive performance, some uncertainties remain. Flood and landslide inventories may contain spatial incompleteness, particularly in remote mountainous areas. In addition,

susceptibility modelling primarily relies on static geomorphic predictors, while dynamic factors such as antecedent rainfall and soil moisture were not explicitly considered. Although spatial cross-validation was used to reduce spatial bias, uncertainty related to DEM resolution and predictor scale may persist. Future work could incorporate higher-resolution terrain data and event-based rainfall information to further improve model reliability.

6 CONCLUSIONS

This study develops an integrated flood–landslide susceptibility framework for the Western Ghats, demonstrating that cascading hazards are governed by the interaction between terrain configuration and extreme rainfall thresholds. Floods and landslides are controlled by distinct but spatially complementary geomorphic drivers, and their co-occurrence intensifies in zones of strong hillslope–channel coupling. By incorporating persistent geomorphic controls into a multi-hazard framework, this approach provides a robust basis for identifying terrain prone to cascading impacts under extreme monsoon events. The methodology offers a transferable foundation for terrain-informed early warning and climate-resilient hazard planning in tropical mountain regions.

ACKNOWLEDGEMENTS

This research was supported by the Department of Science and Technology (DST), Government of India, under the SPLICE–Climate Change Programme (DST/CCP/CoE/140/2018), and by the Green Energy and Sustainability Research Hub (GESH), IIT Bombay (DO/2024-RHUB004-003; Grant No. 0000000000050004495). IIT Bombay provided computational facilities for this study. We acknowledge the India Meteorological Department (IMD) for rainfall datasets and the Geological Survey of India (GSI) for geological and landslide data. Additional geospatial resources were obtained from the Survey of India (SOI) and ESRI.

References

Acosta-Quesada, M., Quesada-Román, A., 2024. Landslides and flood hazard mapping using geomorphological methods in Santa Ana, Costa Rica. International Journal of Disaster Risk Reduction 113, 104882. https://doi.org/10.1016/j.ijdrr.2024.104882

Arango-Carmona, M.I., Voit, P., Hürlimann, M., Aristizábal, E., Korup, O., 2025. Hillslope-Torrential Hazard Cascades in Tropical Mountains. https://doi.org/10.5194/egusphere-2025-1698

Bernard, T.G., Davy, P., Lague, D., 2022. Hydro-Geomorphic Metrics for High Resolution Fluvial Landscape Analysis. JGR Earth Surface 127, e2021JF006535. https://doi.org/10.1029/2021JF006535

Croissant, T., Lague, D., Steer, P., Davy, P., 2017. Rapid post-seismic landslide evacuation boosted by dynamic river width. Nature Geosci 10, 680–684. https://doi.org/10.1038/ngeo3005

Das, S., 2020. Flood susceptibility mapping of the Western Ghat coastal belt using multi-source geospatial data and analytical hierarchy process (AHP). Remote Sensing Applications: Society and Environment 20, 100379. https://doi.org/10.1016/j.rsase.2020.100379

Deijns, A.A.J., Michéa, D., Déprez, A., Malet, J.-P., Kervyn, F., Thiery, W., Dewitte, O., 2024. A semi-supervised multi-temporal landslide and flash flood event detection methodology for unexplored regions using massive satellite image time series. ISPRS Journal of Photogrammetry and Remote Sensing 215, 400–418. https://doi.org/10.1016/j.isprsjprs.2024.07.010

Deroliya, P., Ghosh, M., Mohanty, M.P., Ghosh, S., Rao, K.H.V.D., Karmakar, S., 2022. A novel flood risk mapping approach with machine learning considering geomorphic and socio-economic vulnerability dimensions. Science of The Total Environment 851, 158002. https://doi.org/10.1016/j.scitotenv.2022.158002

Encalada, A.C., Flecker, A.S., Poff, N.L., Suárez, E., Herrera-R, G.A., Ríos-Touma, B., Jumani, S., Larson, E.I., Anderson, E.P., 2019. A global perspective on tropical montane rivers. Science 365, 1124–1129. https://doi.org/10.1126/science.aax1682

Fan, X., Bhuyan, K., Wang, X., Cook, K.L., Ozturk, U., Loew, S., Gyamtsho, P., Jansen, J.D., Xu, Q., 2025. Rethinking policy on high mountain cascading hazards. Nat. Geosci. 18, 1066–1067. https://doi.org/10.1038/s41561-025-01834-w

Hao, L., Rajaneesh A., Van Westen, C., Sajinkumar K. S., Martha, T.R., Jaiswal, P., McAdoo, B.G., 2020. Constructing a complete landslide inventory dataset for the 2018 monsoon disaster in Kerala, India, for land use change analysis. Earth Syst. Sci. Data 12, 2899–2918. https://doi.org/10.5194/essd-12-2899-2020

Ibebuchi, C.C., Abu, I.-O., 2025. Probabilistic flood susceptibility mapping using explainable AI for the Western United States. Environ. Res. Commun. 7, 105008. https://doi.org/10.1088/2515-7620/ae0c5c

IMD, 2021, 2021. Standard operation procedure: weather forecasting and warning services.

Kappes, M.S., Keiler, M., Von Elverfeldt, K., Glade, T., 2012. Challenges of analyzing multi-hazard risk: a review. Nat Hazards 64, 1925–1958. https://doi.org/10.1007/s11069-012-0294-2

Kharismalatri, H.S., Gomi, T., Sidle, R.C., 2025. Geomorphic thresholds for cascading hazards of debris flows and natural dam formation caused by large landslides. Nat Hazards 121, 15537–15552. https://doi.org/10.1007/s11069-025-07402-0

Leonard, M., Westra, S., Phatak, A., Lambert, M., Van Den Hurk, B., McInnes, K., Risbey, J., Schuster, S., Jakob, D., Stafford-Smith, M., 2014. A compound event framework for understanding extreme impacts. WIREs Climate Change 5, 113–128. https://doi.org/10.1002/wcc.252

Li, K., Guo, L., Wang, G., Gao, J., Ma, J., Li, J., Huang, P., Zhai, B., Sun, X., 2025. A novel hybrid framework of high-resolution flood susceptibility mapping in ungauged mountainous regions. Weather and Climate Extremes 50, 100822. https://doi.org/10.1016/j.wace.2025.100822

Liu, L.-L., Duan, C., Gao, J.-H., Xiao, H., Zhu, W.-Q., Yang, C., 2025. Landslide susceptibility assessment using machine learning with a novel SHAP-based sampling strategy. Geoscience Frontiers 102188. https://doi.org/10.1016/j.gsf.2025.102188

Luo, W., Qiu, H., Wei, Y., Huangfu, W., Yang, D., 2025. A proposed method for landslide detection based on transfer learning and graph neural network. Geoscience Frontiers 16, 102171. https://doi.org/10.1016/j.gsf.2025.102171

Mani, P., Allen, S., Evans, S.G., Kargel, J.S., Mergili, M., Petrakov, D., Stoffel, M., 2023. Geomorphic Process Chains in High-Mountain Regions—A Review and Classification Approach for Natural Hazards Assessment. Reviews of Geophysics 61, e2022RG000791. https://doi.org/10.1029/2022RG000791

Mansfield, E.R., Helms, B.P., 1982. Detecting Multicollinearity. The American Statistician 36, 158–160. https://doi.org/10.1080/00031305.1982.10482818

Murphy, K.P., 2013. Machine learning: a probabilistic perspective, 4. print. (fixed many typos). ed, Adaptive computation and machine learning series. MIT Press, Cambridge, Mass.

Pai, D.S., Rajeevan, M., Sreejith, O.P., Mukhopadhyay, B., Satbha, N.S., 2014. Development of a new high spatial resolution (0.25° × 0.25°) long period (1901-2010) daily gridded rainfall data set over India and its comparison with existing data sets over the region. MAUSAM 65, 1–18. https://doi.org/10.54302/mausam.v65i1.851

Pourghasemi, H.R., Kariminejad, N., Amiri, M., Edalat, M., Zarafshar, M., Blaschke, T., Cerda, A., 2020. Assessing and mapping multi-hazard risk susceptibility using a machine learning technique. Sci Rep 10, 3203. https://doi.org/10.1038/s41598-020-60191-3

Pradhan, B., Dikshit, A., Lee, S., Kim, H., 2023. An explainable AI (XAI) model for landslide susceptibility modeling. Applied Soft Computing 142, 110324. https://doi.org/10.1016/j.asoc.2023.110324

Rusk, J., Maharjan, A., Tiwari, P., Chen, T.-H.K., Shneiderman, S., Turin, M., Seto, K.C., 2022. Multi-hazard susceptibility and exposure assessment of the Hindu Kush Himalaya. Science of The Total Environment 804, 150039. https://doi.org/10.1016/j.scitotenv.2021.150039

Tiggeloven, T., Ferrario, D.M., Claassen, J.N., Jäger, W.S., Shapovalova, Y., Koyama, M., De Ruiter, M.C., Daniell, J.E., Torresan, S., Ward, P.J., 2025. A Global Approach for Mapping Multi-Hazard Susceptibility Using Deep Learning: A Case Study in Japan. Artificial Intelligence for the Earth Systems 4, 250039. https://doi.org/10.1175/AIES-D-25-0039.1

Tripathy, S.S., Vittal, H., Karmakar, S., Ghosh, S., 2020. Flood risk forecasting at weather to medium range incorporating weather model, topography, socio-economic information and land use exposure. Advances in Water Resources 146, 103785. https://doi.org/10.1016/j.advwatres.2020.103785

Ullah, K., Wang, Y., Fang, Z., Wang, L., Rahman, M., 2022. Multi-hazard susceptibility mapping based on Convolutional Neural Networks. Geoscience Frontiers 13, 101425. https://doi.org/10.1016/j.gsf.2022.101425

Waleed, M., Sajjad, M., 2025. Advancing flood susceptibility prediction: A comparative assessment and scalability analysis of machine learning algorithms via artificial intelligence in high-risk regions of Pakistan. J Flood Risk Management 18, e13047. https://doi.org/10.1111/jfr3.13047

Wang, Y., Fang, Z., Hong, H., Peng, L., 2020. Flood susceptibility mapping using convolutional neural network frameworks. Journal of Hydrology 582, 124482. https://doi.org/10.1016/j.jhydrol.2019.124482

Youssef, K., Shao, K., Moon, S., Bouchard, L.-S., 2023. Landslide susceptibility modeling by interpretable neural network. Commun Earth Environ 4, 162. https://doi.org/10.1038/s43247-023-00806-5

Zhang, Z., Liu, M., Tan, Y.J., Walter, F., He, S., Chmiel, M., Su, J., 2024. Landslide hazard cascades can trigger earthquakes. Nat Commun 15, 2878. https://doi.org/10.1038/s41467-024-47130-w